

**ARTICLE**

# Analysis and Monitoring of Changes in the Central Marshland Area of Southern Iraq Utilizing Remote Sensing Techniques

Emad Ali Al-Helaly <sup>1\*</sup>, Israa J. Muhsin <sup>2</sup>, Ebtesam F. Khanjer <sup>2</sup>, Ban A. Alrazaq <sup>2</sup>, Sundus A. Abdullah Albakry <sup>2</sup>

<sup>1</sup> Faculty of Engineering, University of Kufa, Al-Najaf 54001, Iraq

<sup>2</sup> Department of Remote Sensing and GIS, College of Science, Baghdad 10001, Iraq

**ABSTRACT**

The marshes of southern Iraq are of great value due to their roles in the economy, environment, heritage, tourism, and agriculture. However, the region has witnessed remarkable transformations in land cover, influenced by human interventions and natural environmental factors. In this research, the Central Marshlands were selected for study and monitoring. These Marshes form the Mesopotamian Marshes, a vital part of the Tigris-Euphrates river system. This area formerly covered an area of approximately 3,000 km<sup>2</sup> and was once home to the lives of Marsh Arabs and their animals. The primary objective of this study was to compile a set of satellite images covering the same marshland region over several decades. The data used includes images captured by various Landsat missions: MSS (1975), TM (1983 & 1993), ETM+ (2003), and the Operational Land Imager (OLI) from Landsat 8 (2015). Satellite images were combined and pre-processed through steps such as layer stacking to create composite images from multiple bands. Several image classification methods were applied, and the classification results showed a significant and unprecedented increase in the percentage of water in the marsh, reaching 16% in 2003. This was combined with vegetation identification techniques, including the identification of vegetation boundaries to detect areas of dense vegetation. In addition, the relative depth of the water was measured to estimate marsh water levels, with the best result obtained in 2003. The normalized mean vegetation index (NDVI) calculated in this study had its best value in 1984 due to the spread of reeds and papyrus during this period. Papyrus is the raw material in the sugar industry, providing a significant economic boost.

**Keywords:** Marshland; Image Classification; NDVI; Vegetation Delineation; Relative Water Depth

**\*CORRESPONDING AUTHOR:**

Emad Ali Al-Helaly, Faculty of Engineering, University of Kufa, Al-Najaf 54001, Iraq; Email: imada.alhilali@uokufa.edu.iq

**ARTICLE INFO**

Received: 12 June 2025 | Revised: 16 June 2025 | Accepted: 25 June 2025 | Published Online: 19 August 2025

DOI: <https://doi.org/10.30564/re.v7i4.9866>

**CITATION**

Al-Helaly, E.A., Muhsin, I.J., Khanjer, E.F., et al., 2025. Analysis and Monitoring of Changes in the Central Marshland Area of Southern Iraq Utilizing Remote Sensing Techniques. *Research in Ecology*. 7(3): 296–301. DOI: <https://doi.org/10.30564/re.v7i4.9866>

**COPYRIGHT**

Copyright © 2025 by the author(s). Published by Bilingual Publishing Group. This is an open access article under the Creative Commons Attribution-NonCommercial 4.0 International (CC BY-NC 4.0) License (<https://creativecommons.org/licenses/by-nc/4.0/>).

# 1. Introduction

The uninhabited, remote, and often extremely inaccessible nature of certain land-cover types—such as dense tropical forests, rugged mountain ranges, expansive deserts, vast stretches of natural vegetation, and large marine and coastal areas—presents significant limitations for collecting accurate, consistent, and comprehensive ground-based statistics and direct observational data. These regions frequently lack human settlements, roads, or infrastructure, making them logistically difficult, dangerous, or economically impractical to access regularly for scientific surveys or monitoring efforts. In some cases, political instability or environmental hazards, such as extreme weather or wildlife, can further complicate data collection. As a result, large portions of the Earth's surface remain poorly studied or underrepresented in traditional datasets, leaving critical knowledge gaps about how these areas are changing in response to natural processes and human-induced pressures such as climate change, resource exploitation, and population expansion. This lack of accessible data limits the ability to make informed decisions regarding land management and conservation strategies, which are essential for sustainable development in many of these regions.

Given these challenges, there has been a significant and ongoing shift toward utilizing remotely sensed data as a primary means of observing, measuring, and analyzing the Earth's surface. Remote sensing involves the use of sensors mounted on aircraft or, more commonly, satellites orbiting the planet, which capture images and other forms of data, such as thermal, radar, and multispectral information, across a wide range of spatial and temporal scales. These sensors can monitor even the most isolated and vast land areas on a consistent basis, enabling the collection of repeatable, long-term datasets that would otherwise be impossible or highly impractical to obtain. This approach not only provides a bird's-eye view of global and regional landscapes but also allows for the early detection of patterns and trends that may indicate environmental degradation or ecological change. Increasingly, the ability to monitor land-cover and land-use changes through satellite observation has become an essential tool for addressing challenges like desertification, deforestation, and wetland loss, providing valuable insights into both the causes and

impacts of these changes <sup>[1-4]</sup>.

The Iraqi Marshlands, including the Central (Qurna), Hawizeh, and Hammar Marshes, collectively forming the Mesopotamian Marshes (see **Figure 1(a)**), are of immense ecological, cultural, social, and economic importance. Recognized as one of the most biodiverse ecosystems in the Middle East, these wetlands serve as a critical habitat for migratory birds and endemic species (see **Figure 1(b)**), while also sustaining the traditional livelihoods of the Marsh Arabs. For centuries, these communities have depended on the marshes for water buffalo rearing, rice cultivation, and fishing, with their unique cultural identity deeply intertwined with the wetland environment. However, the marshlands face significant threats from human activities and environmental changes, including upstream dam construction, water diversion projects, and climate variability. These factors have contributed to drastic alterations in water levels, vegetation cover, and overall ecosystem health. Beyond their cultural value, the marshes play a vital role in climate regulation, carbon sequestration, and supporting livestock production, particularly buffalo grazing, which relies on nutrient-rich aquatic vegetation such as reeds and papyrus. To assess these changes, this study employs remote sensing techniques (see **Table 1**), analyzing a time series of satellite imagery spanning several decades. By processing and classifying these images, the research identifies key trends in land cover, water extent, and vegetation density, providing insights into the marshlands' ecological transformations. The findings contribute to a deeper understanding of the marshes' resilience and vulnerability, offering valuable data for conservation and sustainable management efforts.

**Table 1.** The details and information about the satellites used in image capturing.

Original Images	Conversion from Gaussian and CGS EMU to SI
Marshes (1975)	Landsat 1-5 Multi-Spectral Scanner (MSS) 28-Jul-1973
Marshes (1993)	Landsat 4-5 Thematic Mapper (TM) 28- Jul-1993
Marshes (2003)	Landsat 7 Enhanced Thematic Mapper Plus (ETM+) Scan Line Corrector on (SLC-On)_1999-2003, 29- May- 2003
Marshes (2015)	Landsat 8 OLI (Operational Land Imager) and TIRS (Thermal Infrared Sensor), 27-Sep-2015

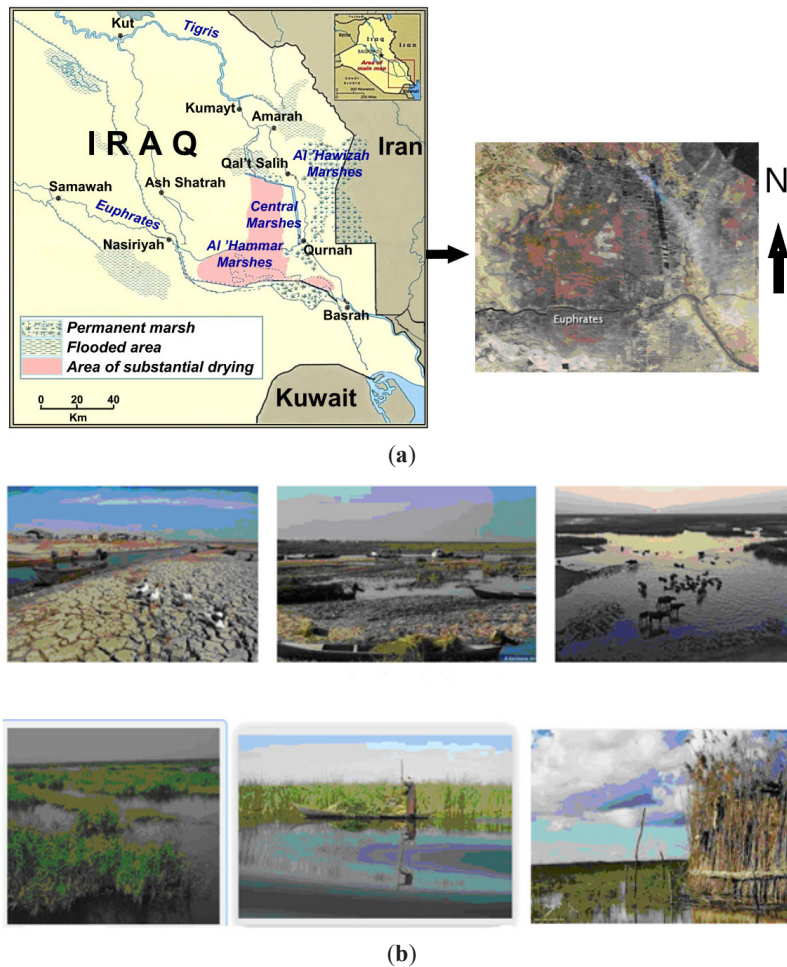


**Figure 1.** (a) The studied area “central marshes southern Iraq”; (b) Some natural pictures of the studied area.

## 2. Materials and Methods

Five satellite images were collected using different sensors, each from different periods to capture various stages of environmental change and land-cover dynamics across the study area. The specific satellites and sensors used are as follows:

- i. Landsat MSS (1975): This is the earliest image from the Landsat Multi-Spectral Scanner (MSS), which offers moderate-resolution imagery in four spectral bands. It provides valuable insight into land-cover changes from the mid-1970s.
- ii. Landsat Thematic Mapper TM (1983 and 1993): This sensor, an upgrade to MSS, provided enhanced capabilities, including seven spectral bands and better spatial resolution. It allowed for more detailed observation of land cover changes and vegetation health during the late 1980s and early 1990s.

- iii. Landsat 7 Enhanced Thematic Mapper Plus ETM+ (2003): With its improved spatial and radiometric resolution, the ETM+ sensor offered higher accuracy for monitoring land-use and land-cover changes at a finer scale, making it ideal for tracking alterations in the marshes and surrounding areas.

- iv. Landsat 8 Operational Land Imager (OLI) and Thermal Infrared Sensor (TIRS) (2015): The most recent satellite image combines the OLI for high-resolution visible, near-infrared, and shortwave infrared bands and the TIRS for thermal infrared data. This sensor suite provided comprehensive coverage, allowing for more precise monitoring of temperature changes, water distribution, and vegetation dynamics across the marshlands.

All the images collected from these various Landsat sensors cover the study area (see **Figure 2**), which includes the southern Iraq marshes, and require rectification

and calibration to ensure accurate comparisons over time. The rectification process aligned the images to geographic coordinates, ensuring that they could be overlaid and compared accurately, while calibration helped account for atmospheric effects and sensor-specific errors. The study area focuses on the Central Marshes, a vital ecological region located at the confluence of the Tigris and Euphrates rivers, which forms the core of the Mesopotamian wetland ecosystem. Geographically, the marshes are bounded by

the Euphrates River to the south and the Tigris River to the east, with the area forming a rough triangular shape between the cities of Al-Nasiriyah, Qalat Saleh, and Al-Qurnah. This positioning is crucial, as the marshes act as an interface between the two great rivers, receiving water primarily from the distributaries of the Tigris River -specifically the Shatt-al-Muminah and Majar-al-Kabir branches- and from the Euphrates River along their southern boundary.

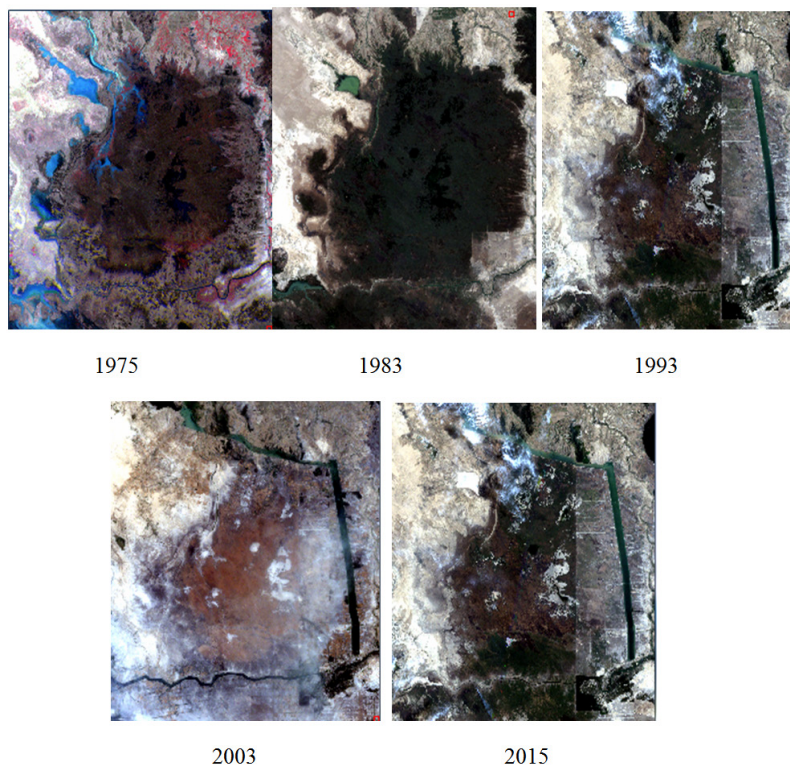


**Figure 2.** The five original images of the studied area were captured in different periods.

Covering an area of approximately 3,000 km<sup>2</sup>, the Central Marshes are subject to seasonal fluctuations in water coverage, expanding to over 4,000 km<sup>2</sup> during flood periods. These wetlands are of immense ecological importance, as they serve as a critical habitat for a wide variety of species, especially waterfowl. They act as a vital breeding, aggregation, and wintering habitat for numerous migratory waterfowl species, which rely on the marshes for food, shelter, and nesting. The biodiversity supported by the marshes is essential for maintaining the ecological health of the region, providing services such as flood mitigation, groundwater recharge, and carbon sequestration. These ecosystems are integral to both local and regional environmental sustainability, as well as to the livelihoods

of people who rely on them for agriculture and fishing <sup>[5,6]</sup>.

The study area is geographically located with the upper left coordinates at 662,640.00E, 3,493,710.00N, and the lower correct coordinates at 733,230.00E, 3,415,350.00N, by the Universal Transverse Mercator (UTM) coordinate system. These precise coordinates help define the exact boundaries of the marshland areas under observation and provide a foundation for spatial analysis and interpretation of the satellite imagery collected across different periods.

## 2.1. Image Rectification

Rectifying Landsat imagery is a crucial step to ensure that satellite images align accurately with real-world



coordinates, making spatial analysis more reliable. The process begins by creating an ortho-rectified base image, which corrects distortions caused by sensor angle, terrain variations, and atmospheric conditions. This results in a map-like image that serves as a reference for aligning other photos. In the next step, all additional pictures are geometrically adjusted to match this base using the PCI OrthoEngine and its precise orbital modeling tools, ensuring consistent alignment across different periods and sensors. Ground Control Points (GCPs) are then identified and matched using cross-correlation techniques to fine-tune the accuracy. To ensure high precision, the final output undergoes both visual checks and automated similarity assessments—an essential step for applications like land cover analysis and monitoring changes over time <sup>[4]</sup>.

## 2.2. Image Calibration

Ideally, in remote sensing, calibrating satellite images to standard reflectance units is essential for making accurate and consistent comparisons across different times and sensors. While full calibration is ideal, many change detection studies often use a more straightforward method—normalizing the raw digital numbers (DN) to match a reference image. This approach is usually sufficient for identifying changes in land cover. Radiometric correction generally involves adjusting for atmospheric conditions, sensor variations, and geometric distortions. One crucial step in this process is Top-of-Atmosphere (TOA) reflectance calibration, which accounts for changes in the Earth-sun distance and solar angle. These factors affect how much sunlight is reflected off the Earth's surface, so correcting for them improves the reliability of comparing images taken under different lighting conditions or at other times <sup>[4-7]</sup>.

The TOA reflectance calibration procedure involves a specific calculation that incorporates the following key variables:

1. The sun zenith angle for each pixel in the image represents the angle between the Sun and the vertical line from a given point on the Earth's surface.
2. The sun azimuth angle for each pixel describes the direction of the Sun relative to the North, essentially providing information about the Sun's position in the sky at the time the image was captured.
3. The distance from the scene center to the Sun changes throughout the year as the Earth orbits the Sun. This

distance is important because it affects the amount of solar radiation that reaches the Earth's surface.

Radiometric calibration is a key step in accurately interpreting Landsat images. It corrects for variations in solar angles and the Earth-sun distance across the scene, ensuring consistent brightness and reflectance values. Each spectral band—whether in the visible, near-infrared, or thermal infrared range—is calibrated separately to maintain accuracy. Adjusting the raw digital values based on solar geometry reduces the impact of environmental and sensor-related factors. Radiometric calibration is essential for comparing images over time or across different locations, as it ensures reliable results for land cover change detection and enhances the overall quality of the analysis <sup>[8]</sup>.

## 2.3. Image Classification

“Image classification” is a fundamental process in remote sensing and computer vision that aims to automatically categorize all pixels in a digital image into distinct, meaningful classes based on their spectral, spatial, and contextual attributes. This process relies on spectral signatures, unique patterns of electromagnetic energy reflected or emitted by different surface materials, which serve as fingerprints to distinguish one land cover type from another. These signatures are derived from multispectral or hyperspectral sensor data, where each pixel's reflectance values across different wavelengths define its class membership. The classification process is critical for applications such as land cover mapping, environmental monitoring, urban planning, and agricultural assessment.

There are two primary methodological approaches to image classification: supervised classification (the method adopted in this research) and unsupervised classification, each with distinct advantages and limitations. Unsupervised classification is a data-driven approach that identifies inherent spectral categories within an image without requiring prior knowledge of land cover types. This method typically employs clustering algorithms, such as k-means or ISODATA, which group pixels based on their spectral similarity in feature space. These techniques iteratively estimate the spectral category of each pixel while simultaneously determining the optimal number of spectral clusters and their spatial distribution within the dataset <sup>[9,10]</sup>. Unsupervised classification is beneficial for exploratory analysis when ground truth data is unavailable or when the

spectral characteristics of the study area are unknown.

In contrast, supervised classification, the most widely used approach for quantitative remote sensing analysis, leverages pre-existing knowledge to train algorithms that assign each pixel to a predefined set of land cover categories. This method requires representative training samples -collected from field surveys, high-resolution imagery, or existing maps- to teach the classifier how different land cover types manifest spectrally. A diverse range of algorithms is available for supervised classification, including parametric methods that model the probability distribution of spectral data for each class (e.g., Gaussian maximum likelihood) and non-parametric techniques that partition the multispectral feature space using decision boundaries (e.g., support vector machines, random forests, or artificial neural networks)<sup>[11]</sup>. The choice of algorithm depends on factors such as data dimensionality, class separability, and

computational efficiency.

In this study, we employed two robust supervised classifiers -the Mahalanobis distance classifier and the maximum likelihood classifier (MLC)- to categorize the study area into four distinct land cover classes: water, vegetation, soil, and dry soil. The Mahalanobis distance classifier is a statistical method that accounts for covariance between spectral bands, making it effective for distinguishing classes with overlapping spectral responses. Meanwhile, MLC assumes a Gaussian distribution of training data and calculates the probability of a pixel belonging to each class, assigning it to the most likely category. The classification results, presented in **Figures 3** and **4**, demonstrate the spatial distribution of land cover across the study area. In contrast, **Figures 5** and **6** provide detailed statistical distributions of pixel values for each class, highlighting their spectral separability and classification accuracy.

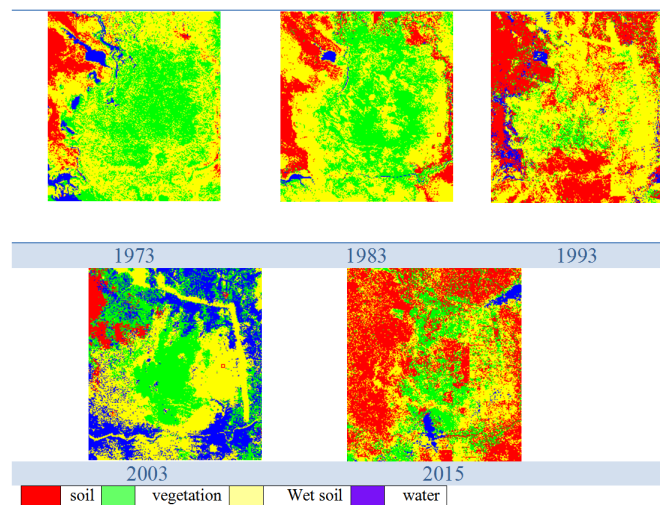


**Figure 3.** The classification results using the Mahalanobis classifier.

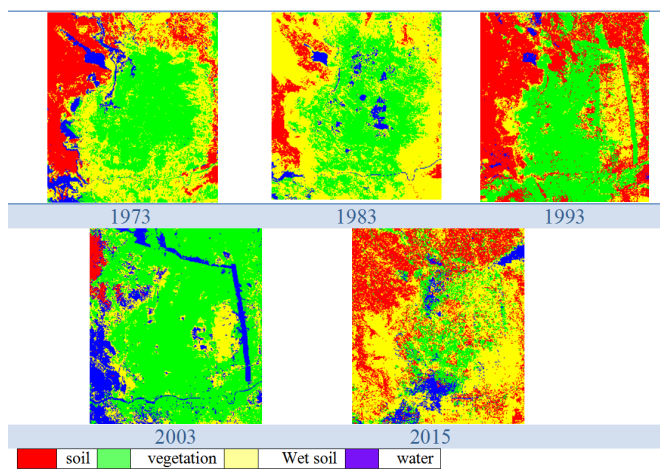


**Figure 4.** The classification results using a maximum likelihood classifier.

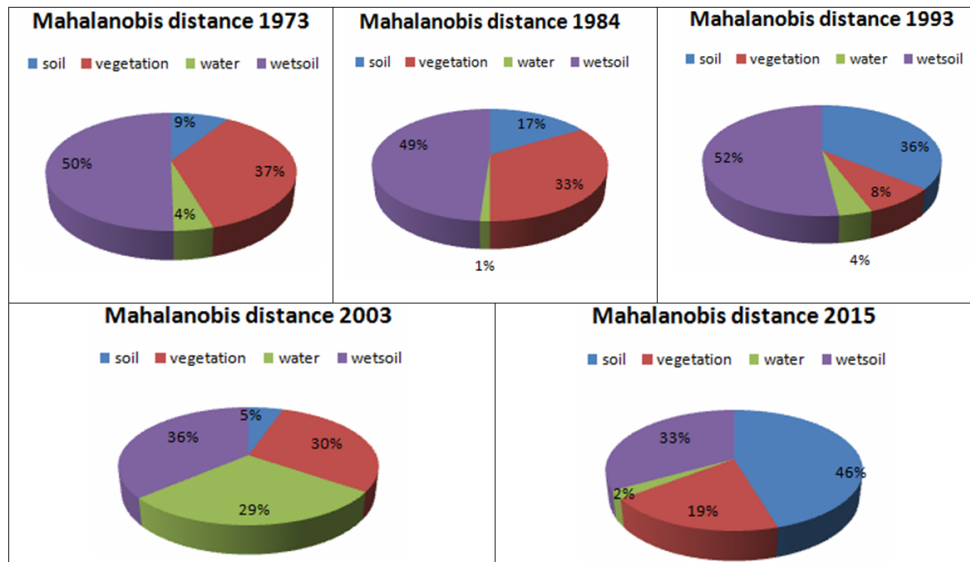


Figure 5. The statistical distribution of the Mahalanobis classifier in different periods.

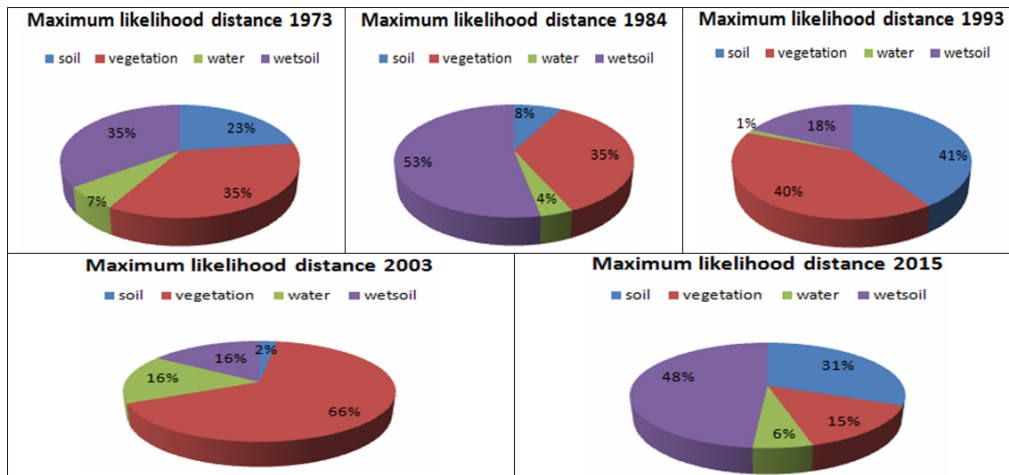


Figure 6. The statistical distribution of the Maximum likelihood classifier in different periods.

## 2.4. Monitoring the Vegetation Using NDVI

The Normalized Difference Vegetation Index (NDVI) is the most widely used satellite-derived spectral index for assessing vegetation health, density, and photosynthetic activity on a global scale <sup>[12,13]</sup>. As a standardized metric, NDVI quantifies the presence and vigor of green vegetation by exploiting the distinct spectral reflectance characteristics of chlorophyll-rich plant leaves across different wavelengths.

Healthy, dense vegetation exhibits strong chlorophyll absorption in the visible red band (RED, ~600–700 nm) while reflecting a significant portion (typically 25–50%) of near-infrared radiation (NIR, ~700–1100 nm) due to the in-

ternal scattering of light by leaf cell structures. In contrast, stressed, sparse, or non-photosynthetic vegetation reflects more red light (due to reduced chlorophyll absorption) and less NIR radiation (due to disrupted cell structures or reduced leaf area). Bare soil, urban areas, and water bodies exhibit distinctly different reflectance patterns, with soils often showing moderate reflectance in both bands and water absorbing most NIR and red wavelengths.

The NDVI is calculated as a normalized ratio of the difference between NIR and red reflectance to their sum, expressed by the formula <sup>[14]</sup>:

$$NDVI = \frac{NIR - RED}{NIR + RED} \quad (1)$$

This index ranges from -1 to +1, where:

- i. Values  $> 0.6$  indicate dense, healthy vegetation (e.g., forests, crops in peak growth).
- ii. Values  $0.2\text{--}0.5$  represent moderate vegetation (grasslands, agricultural fields).
- iii. Values near 0 suggest bare soil or non-vegetated surfaces.
- iv. Negative values typically correspond to water bodies (due to higher red reflectance than NIR).

NDVI's simplicity, robustness, and sensitivity to vegetation dynamics make it indispensable for applications like crop monitoring, drought assessment, deforestation tracking, and climate change studies<sup>[12,13]</sup>. However, limitations include saturation effects in dense canopies and sensitivity to atmospheric conditions, prompting the development of enhanced indices like EVI (Enhanced Vegetation Index) for specific use cases.

The vegetation index is calculated using reflectance values from near-infrared and red spectral bands. The NDVI values typically range from  $-1$  to  $1$ , where: Increasing positive values indicate greater vegetation density and

health, and Negative values represent non-vegetated surfaces (water, barren land, ice, snow, or clouds). NDVI data are typically used for qualitative comparisons, either to monitor vegetation changes over time or to compare different regions with similar characteristics<sup>[15–21]</sup>.

In this study, NDVI was employed to distinguish between healthy and unhealthy vegetation within the research area. The results of this analysis are presented in **Figure 7**.

## 2.5. Vegetation Delineation

Vegetation identification or delineation can be used to detect plant presence and visualize vegetation vigor quickly. The analysis software provides tools to generate graphics for reports and presentations easily. Each image represents a specific period in Karbala's seasonal cycle, categorized into four distinct seasons. The NDVI produces values ranging from  $-1.0$  to  $1.0$ . Pixels with no NDVI value between  $-1.0$  and  $0.249$ , whereas pixels with strong vegetation tend to be  $1.0$ . The results of the vegetation mapping analysis are presented in **Figure 8**.

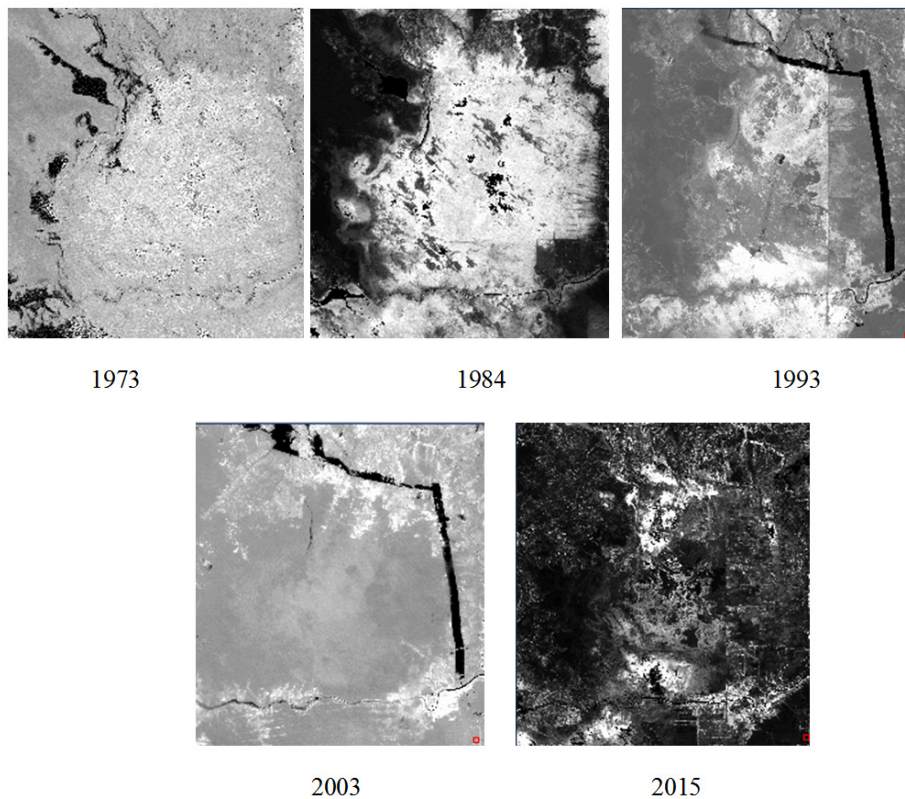


**Figure 7.** The results of NDVI applied to different periods.



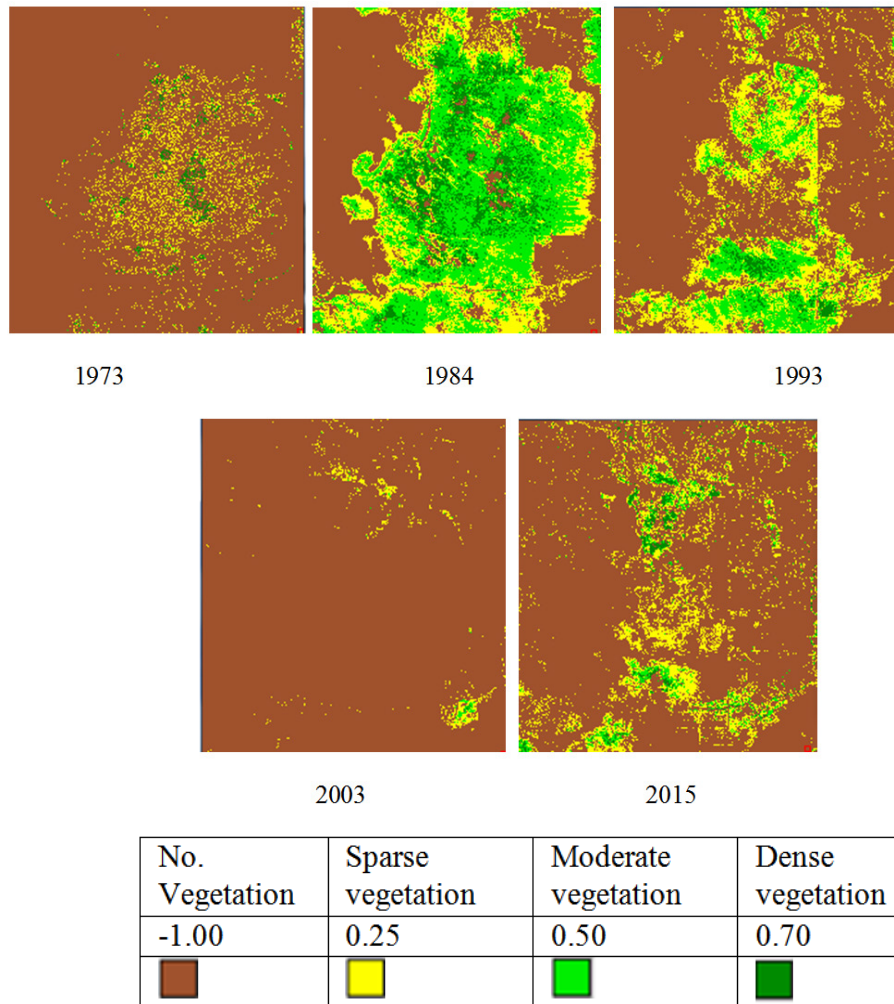


**Figure 8.** The results of vegetation delineation for the center marsh image in different periods.

## 2.6. Relative Water Depth

Relative Water Depth (RWD) is a remote sensing technique that estimates water depth in lakes, rivers, and oceans by analyzing light attenuation through the water column. This method is essential for bathymetric mapping, environmental monitoring, coastal management, and water depth/height estimation<sup>[22–24]</sup>. The optical principles underlying this technique can be summarized as:

- i. Water absorbs and scatters light differently across various wavelengths
- ii. Shorter wavelengths (blue/green spectrum) penetrate deeper than longer wavelengths (red/near-infrared)
- iii. The reflectance ratio between different wavelengths correlates with water depth

Lyzenga D. R. (1981)<sup>[21]</sup> developed a semi-analytical approach based on radiative transfer theory that accounts

for water's optical properties. This work established the fundamental equation for calculating Relative Water Depth (RWD):

$$\ln(L(\lambda_i) - L_\infty(\lambda_i)) = a_i + b_i \cdot d \quad (2)$$

Where:

- $L(\lambda_i)$  : radiance at wavelength  $\lambda_i$
- $L_\infty(\lambda_i)$ : deep-water radiance
- $a_i, b_i$ : coefficients related to water attenuation
- $d$ : water depth

Satellites such as Landsat (TM/ETM+/OLI), Sentinel-2 (MSI), and MODIS provide excellent data sources for this technique. The method yields optimal results in clear, shallow waters (20–30 meters depth), though reflections from seabed features like sand and seagrass may affect results<sup>[21]</sup>. **Figure 9** demonstrates the application results of this technique.

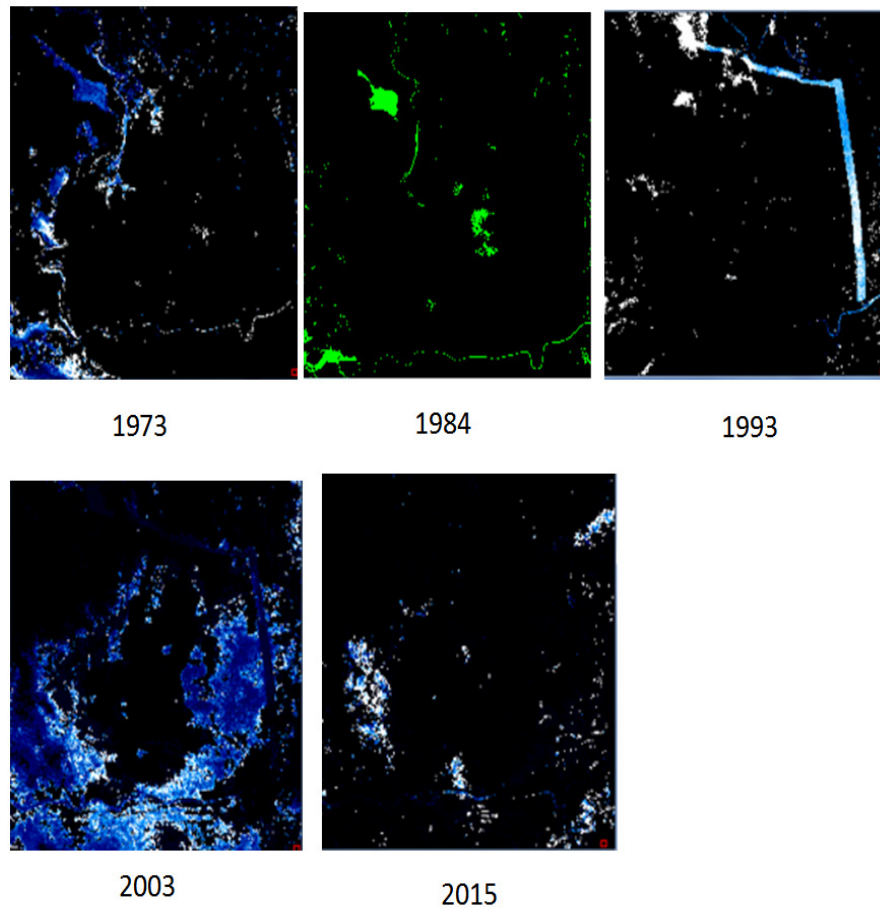


**Figure 9.** The results of applying the relative water depth technique on the studied area for the period (1973–2015).

## 2.7. Relative Water Depth (RWD) Limitations

Remote depth measurement (RWD) methods rely heavily on the optical penetration of light into water bodies. In turbid or sediment-laden waters, light may not penetrate deeply enough, reducing the accuracy of depth estimates. Areas with high suspended sediments, plankton, or colored dissolved organic matter (CDOM) can distort reflectance signals. Surface conditions, such as sun glare, waves, or wind-induced undulation, can introduce noise into RWD images, affecting the quality and consistency of RWD calculations.

Sensor accuracy, radiosensitivity, and atmospheric correction errors can affect the accuracy of deep-water measurements. So this method is most effective in shallow water (typically less than 20 meters), where light can penetrate the bottom. Deep water tends to absorb most of the light, making deep-water measurements unreliable beyond this range <sup>[25]</sup>.

## 3. Results and Discussion

Changes in the central marshes of Iraq have had significant social and economic impacts on local communities. As water levels fell, many were forced to leave their homes, losing traditional livelihoods such as fishing, herding, and collecting reeds. This led to widespread poverty, reduced access to clean water, and deteriorating health conditions. Access to education and basic services became more difficult, and the unique Marsh Arab culture began to disappear. Women were particularly affected, facing greater challenges due to the loss of income and increased responsibilities.

The Central Marshes of Iraq represent an ecologically significant area. This research provides a comprehensive study and detailed analysis of land cover classes (soil, wet soil, vegetation, and water) using two supervised classification methods. The results of the first technique, “Mahalanobis Distance Classifier,” show that the percentage

rate of class soil and wet soil together was 59% for 1973, 66% for 1984, 88% for 1993, 66% for 2003, and 79% for 2015. It can be noticed that the maximum rate of soil class was recorded for 1993, compared with the water and the vegetation, which had decreased because of the policies followed by the previous government, where the water had been cut off. The marshes had been drained, which led to desertification of the area. As for the water category, we note that the highest classification rate was in 2003, due to the reflow of water into the marshes, which led to the recovery of the marshes and filling them with water during this period. As for the variety of crops or vegetation classes, we notice a decrease in the amount that occurred in 1993 due to the lack of water after the process of draining the marshes.

Regarding the second classification method employed in this research, the statistical distribution of classified land cover categories revealed the following patterns: the proportion of the soil class with wet soil was 58% for 1973, 61% for 1984, 59% for 1993, 68% for 2003, and 68% for 2015. There is some convergence between the two classification methods in terms of soil and wet soil ratio. On the other hand, the results of the statistical distribution show that the maximum value of vegetation was recorded in 2003 according to the second classification method.

NDVI analysis revealed the highest values (approaching 1) in 1984, indicating robust agricultural recovery with crops like reeds and rice. Vegetation delineation results corroborated these findings, with 1984 images showing significantly greener and brighter areas compared to other years.

Comparative analysis suggests the Mahalanobis classifier provides more realistic results than the Maximum Likelihood approach. Both methods indicate declining water percentages, attributable to climate change impacts, including reduced rainfall and increased temperatures.

It is noted that the relative water depth (RWD) technique achieves good results in swamp areas due to their shallow nature. Several factors can affect the values measured using this method, including plankton and algae present at the bottom of the swamp, which affect the reflected wavelengths. Water turbidity and the proportion of mud and sediment present in swamp water can also negatively affect the measured values.

Despite these limitations, RWD has gained recognition as a valuable method and is now implemented in major remote sensing software packages like ENVI and ArcGIS.

## 4. Conclusions

This should clearly explain the main conclusions of the article, highlighting its importance and relevance. The study of the Central Marsh in southern Iraq has provided insight into the significant land cover changes that have occurred over several decades due to both human activities and natural conditions. By utilizing a time series of Landsat satellite imagery (1975–2015), this research tries to submit a periodic monitoring and analysis of the variations in vegetation cover, water extent, and marshland health through advanced remote sensing techniques, including NDVI analysis, water depth estimation, and vegetation boundary identification. The results highlight the crucial transformations in the marshlands, emphasizing the impacts of water management policies, climate variability, and human intervention on this culturally and ecologically vital region. The findings underscore the urgent need for sustainable management strategies to conserve and restore the Mesopotamian Marshes, ensuring their ecological functions and the livelihoods of local communities.

This research helps in a deeper understanding and more accurate monitoring of the dynamics of marshlands in southern Iraq and provides a foundation for future conservation efforts. Further studies incorporating higher-resolution imagery and ground-based validation could enhance the accuracy of monitoring systems, supporting more effective policy decisions for the protection of this critical wetland ecosystem.

## Author Contributions

All researchers participated in various works and contributed to all parts of the research, all of them have read and agreed to the published version of the manuscript.

## Funding

This research received no external funding.

## Institutional Review Board Statement

Not applicable.

## Informed Consent Statement

Not applicable.

## Data Availability Statement

No new data were created.

## Conflict of interest

The authors declare no conflict of interest.

## References

- [1] Lillesand, T., Kiefer, R.W., Chipman, J., 2004. Remote sensing and image interpretation. John Wiley & Sons: Hoboken, NJ, USA.
- [2] Diallo, Y., Hu, G., Wen, X., 2009. Applications of remote sensing in land use/land cover change detection in Puer and Simao Counties, Yunnan Province. *Journal of American Science*. 5(4), 157–166.
- [3] Forkuo, E.K., Frimpong, A., 2012. Analysis of forest cover change detection. *International Journal of Remote Sensing Applications*. 2(4).
- [4] Symeonakisab, E., Caccettab, P.A., Wallaceb, J.F., et al., 2006. Multi-temporal land use/cover change detection in the Spanish Mediterranean coast. 34(Part XXX).
- [5] UNEP, Partow, H., 2001. The Mesopotamian Marshlands: Demise of an Ecosystem.
- [6] Scott, D.A., 1995. A directory of wetlands in the Middle East. IUCN.
- [7] Wu, X., Caccettab, P.A., Furby, S.L., et al., 2005. Remote Sensing Analysis of Land Cover Change. In: *Proceedings of International Symposium on Spatio-temporal Modelling, Spatial Reasoning, Spatial Analysis, Data Mining and Data Fusion*. *Journal of Environmental Sciences, Beijing*. 327–332.
- [8] Vermote, E., Tanré, D., Deuzé, J.L., et al., 1994. Second Simulation of the satellite signal in the solar spectrum (6S), 6S User Guide Version 0. NASA-Goddard Sp. Flight Center-Code. 923.
- [9] Richards, J.A., Jia, X., 1999. Remote sensing digital image analysis. Springer. pp. 3.
- [10] Stathakis, D., Vasilakos, A., 2006. Comparison of Computational Intelligence Based Classification Techniques for Remotely Sensed Optical Image Classification. *IEEE Transactions on Geoscience and Remote Sensing*. 44(8), 2305–2323.
- [11] Muhsin, I.J., 2011. Al-Hawizeh Marsh Monitoring Method Using Remotely Sensed Images. *Iraqi Journal of Science*. 52(3), 381–387.
- [12] Bellone, P.B., Bellone, F.P.T., 2009. Investigation of Vegetation Dynamics using Long-Term Normalized Difference Vegetation Index Time-Series. *American Journal of Environmental Sciences*. 5(4), 460–466.
- [13] Pierce, F.J., Clay, D., 2006. GIS Applications in Agriculture. 41–42.
- [14] Gandhi, M., Parthiban, G.S., Nagaraj, T., et al., 2015. NDVI: Vegetation change detection using remote sensing and GIS –A case study of Vellore District. *Procedia - Procedia Computer Science*. 57, 1199–1210.
- [15] Chen, X., Vierling, L., Deering, D., 2005. A simple and effective radiometric correction method to improve landscape change detection across sensors and across time. *Remote Sensing of Environment*. 98, 63–79.
- [16] Yacoub, D., Guangdao, H., Xingping, W., 2010. Assessment of Land Use Cover Changes Using NDVI and DEM in Puer and Simao Counties, Yunnan Province, China. *Report and Opinion*. 2(9), 7–16.
- [17] Muhsin, I.J., Hamid, A., 2017. Monitoring the Changes of Vegetal Cover of Karblaa Province (Iraq) using Target Detection and Classification Techniques. *International Journal of Science and Research*. 6(7), 1408–1412.
- [18] Muhsin, I.J., 2016. Change detection of remotely sensed image using NDVI subtractive and classification methods. *Iraqi Journal of Physics*. 14(29), 125–137.
- [19] Hussain, H.A., Abdullah, S.A., Al Maliki, A.A., 2023. Using spatial analysis methods to evaluate the soil contamination of Baghdad city, Iraq. *Journal of Physics: Conference Series*. 2114.
- [20] Mahdi, F., Adul Razzaq, B., Sultan, M., 2023. Assessment of Satt al-ara water quality using CCME/WQI analysis in Basrah city of south Iraq. *Iraqi Journal of Science*. 64(1), 480–491.
- [21] Hassan, Z.D., 2025. Geomorphological and Environmental Characteristics of the Al-Mashab and Al-Salal Marshes, Southern Iraq. *Iraqi Journal of Science*. 66(3), 1095–1108. DOI: <https://doi.org/10.24996/ijs.2025.66.3.10>
- [22] Lyzenga, D.R., 1981. Remote sensing of bottom re-



- flectance and water attenuation parameters in shallow water using aircraft and Landsat data. *International Journal of Remote Sensing*. 2(1), 71–82. DOI: <https://doi.org/10.1080/01431168108948342>
- [23] Stumpf, R.P., Holderied, K., Sinclair, M., 2003. Determination of water depth with high-resolution satellite imagery over variable bottom types. *Limnology and Oceanography*. 48(1-part-2), 547–556. DOI: <https://doi.org/10.4319/lo.2003.48.1-part-2.0547>
- [24] Pacheco, A., Horta, J., Loureiro, C., Ferreira, Ó., 2015. Retrieval of nearshore bathymetry from Landsat 8 images: A tool for coastal monitoring in shallow waters. *Remote Sensing of Environment*. 159, 102–116. DOI: <https://doi.org/10.1016/j.rse.2014.12.004>
- [25] Losada, M.Á., 2021. Method to assess the interplay of slope, relative water depth, wave steepness, and sea state persistence in the progression of damage to the rock layer over impermeable dikes. *Ocean Engineering*. 239, 109904.